Proceedings of the Fifteenth International Conference on
Computational Structures Technology
Edited by: P. Iványi, J. Kruis and B.H.V. Topping
Civil-Comp Conferences, Volume 9, Paper 12.1
Civil-Comp Press, Edinburgh, United Kingdom, 2024
ISSN: 2753-3239, doi: 10.4203/ccc.9.12.1

Equilibrium Analysis of 2D Complex Discrete Assemblies Modelled using Cracking Blocks with Non-Dilatant Interfaces

A. Iannuzzo[1], M. Herczeg[2], K. Bagi[2] and E. Mousavian[3]

[1]Department of Engineering, University of Sannio, Benevento, Italy
[2]Department of Structural Mechanics, Budapest University of Technology and Economics, Hungary
[3]Edinburgh School of Architecture and Landscape Architecture (ESALA), The University of Edinburgh, United Kingdom

Abstract

In recent years, innovative computational methods for designing sustainable discrete element assemblies have gained attention, focusing on materials with low carbon footprints and environmentally friendly joinery methods. In particular, dry joints, used to assemble blocks without mortar, can perform minimal environmental impact as reduces material consumption as well as providing sustainable assembling and disassembly processes.
This research introduces Joint Layout Design (JLD), a new 3D computational approach for modelling and assessing discrete element assemblies with complex-shaped, non-planar interfaces. Unlike standard methods that consider blocks as rigid, JLD accounts for potential internal failures by considering finite internal material strengths in tensile and shear modes. The JLD method models potential failure planes within blocks using inner interfaces with a finite tensile and shear strength, while the contact among rigid blocks occurs on dry unilateral interfaces governed by a non-associative Mohr-Coulomb friction law. The mechanical problem is framed as a limit analysis equilibrium problem and solved via interactive second-order cone programming. JLD analyses of 2D mechanical problems are proposed and validated to demonstrate its advantages and limitations, including an analysis of a flat arch inspired by Leonardo's arch, which is benchmarked against the distinct element method in 3DEC.

Keywords: limit analysis, multi-surface plasticity, 3DEC, masonry, load-bearing capacity, non-planar dry interfaces, discrete element, virtual experiment.

1 Introduction

In recent years, there has been a growing interest in designing and manufacturing innovative and sustainable discrete element assemblies. These structures usually aim to use materials with a low carbon footprint, making masonry one of the most popular choices. Additionally, these assemblies benefit from being connected using environmentally friendly joinery methods. Among these methods, dry joints—where blocks are assembled without mortar—are ideal because of their minimal environmental impact.

Finding the ideal joint layout within a discrete assembly has been a long-standing design challenge, resulting in a diverse range of bond patterns and stereotomy techniques throughout history. The dependency of structural behaviour on the joint layout, i.e. shape and location of the joints, has been widely acknowledged and explored in several recent studies, such as [1], which addressed the structural behaviour of different bond patterns, and [2], which examined various stereotomy methods and their impact on load-bearing capacities. However, it can be extensively observed that manufacturing and construction constraints have dominantly been prioritised over structural preferences in the discretisation of structures [3]. Following this trend, most research on contemporary architectural design has focused on addressing construction issues, such as simplifying fabrication by segmenting free forms into primitive and modular geometries [4].

These constraints are gradually being mitigated through digital manufacturing techniques, allowing us to fabricate entities with complex geometries more easily. One argument is that eliminating such construction-oriented limitations enables us to build structures as a whole, as seen with concrete printers. However, segmentation remains crucial for packing, transporting, and assembling structures [5], particularly in compact urban areas with limited construction space, distant locations, or challenging conditions such as constructing bridges over valleys or rivers. When materials like masonry are used, discretising the whole into smaller parts becomes more crucial due to their vulnerability to tensile fractures. Therefore, while segmentation of structures is necessary to facilitate construction, it is now possible to explore segmentation methods and joint layouts that maximise structural performance rather than focusing solely on achieving maximum modularity and planarity of block faces. This represents a new paradigm shift. However, it is important to note that construction-oriented concerns remain significant, particularly in mitigating environmental damage and reducing material waste caused by the Architecture Engineering Construction (AEC) sector.

Masonry blocks with complex geometries can be fabricated using additive, subtractive, and formative methods [6]. Additive manufacturing, such as 3D printing, has enabled the creation of structures from materials like sand [7], earth [8], clay [9], and concrete [10]. However, the final product tends to be non-homogeneous since it is built layer by layer. Subtractive methods, like wire and blade cutting and robotic carving and milling [11], offer an alternative that results in homogeneous blocks.

Using digital stereotomy, these methods can cut relatively homogeneous natural materials like stones into complex geometries. However, material waste remains a significant challenge with these techniques. Formative methods, such as moulding masonry mortars [12, 13], allow for manufacturing homogeneous models with complex geometries and can relatively mitigate material waste, especially when moulds are reusable. However, this process is often time-consuming.

Advances in manufacturing discrete masonry assemblies with complex geometries highlight the need for novel computer-aided design (CAD) frameworks that support designers in exploring the shapes of discrete structures during the early stages of design. Such computational efficiency cannot be achieved through methods like finite element (FE) and discrete element (DE) analyses.

The analysis of discrete assemblies can achieve considerable computational efficiency through certain simplifications, as first proposed by Heyman with his three assumptions based on no-tensile strength, no-sliding and infinite compressive resistance [14]. While the Heyman assumptions were developed to general masonry constructions provided that rules of arts are followed, in [15], Livesey developed a limit state approach to apply limit analysis of assembly composed of rigid blocks considering also sliding among blocks. His method was then specialised into two main approaches, i.e., convex and concave contact models [16]. The convex approach abstracts a joint to a single point at its centre, while the concave approach assumes the contact among the blocks occurs over the vertices of the polygala interface describing the joint's boundary. While both approaches were extended to analyse historic masonry buildings, the concave method has been recently adopted by Kao et al. [17] to design novel discrete assemblies with complex geometries, though the blocks are set as convex polyhedrons with planar faces. Kao et al. [18], later on, in 2022, used a concave formulation to analyse interlocking assemblies with arbitrary non-planar interfaces by abstracting the interface to numerous contact points distributed along the edges of the face. This framework, however, considered the blocks to be fully rigid. In contrast, Mousavian et al. [19] extended the concavity formulation to analyse assemblies composed of fracturable blocks with non-planar contact faces. The possibility of fracture becomes a crucial issue when dealing with blocks with concave polyhedral geometries, commonly seen in interlocking assemblies. Multi-surface plasticity [20] provides a solution by embedding the possibility of block fracture by introducing prescribed potential failure interfaces within the blocks, allowing for the possibility of cracking. This means that the entire assembly is modelled with two sets of potential discontinuities, each with different failure criteria: dry interfaces (joints between blocks) and inner interfaces within each block that may crack. The elements spanning these failure faces are still considered rigid. Portioli et al. [21] modelled conventional masonry walls constructed from cubic bricks arranged in a running bond pattern by adopting the convex approach. This model included inner interfaces along the vertical and horizontal symmetric axes and the diagonals of each block. The primary difference between the inner and dry interfaces was the inclusion of non-zero cohesion at the inner faces.

The present research introduces a new 3D computational approach called Joint Layout Design (JLD) to model and assess discrete element assemblies with crackable blocks having complex-shaped faces, particularly non-planar ones. To develop this

model, standard equilibrium analysis is reformulated and extended to model inner interfaces with finite elastic tensile and shear-torsion strengths. While the specified flow rule at the inner interfaces automatically implies zero dilation, the heuristic procedure proposed by Gilbert et al. [22] is adopted in sequential programming to account for a non-associative Mohr-Coulomb law at the dry joints. The mechanical problem is modelled within the framework of limit analysis using a concave formulation and solved as second-order cone programming. Dual displacements are retrieved and then used to define the failure mechanism. Given a dense set of potential discontinuities that can act as either inner or dry faces, the JLD method allows the investigation of different combinations of inner and dry faces and, thus, explores several possibilities for segmenting a structure. Thus, JLD helps to explore the optimal combination of dry and inner faces corresponding to the maximum load-bearing capacity, as presented with simple examples by Mousavian and Casapulla [23].

The paper is structured as follows. Section 2 presents the JLD method and briefly introduces the distinct element method. Section 3 illustrates a few JLD analyses of simple but meaningful models, including a flat arch inspired by Leonardo that is validated against 3DEC V.7.0 [24]. Lastly, Section 4 outlines the main conclusions.

2 Methods

This Section introduces the JLD method (Section 2.1) and its mathematical programming formulation used to solve the limit-analysis problem. After that, Section 2.2 provides a brief overview of the Distinct (Discrete) Element Method (DEM) and introduces 3DEC—software developed based on DEM principles used for benchmarking results obtained by JLD.

2.1 JLD method

This Section introduces the main features of the JLD method and its numerical implementation. In particular, Section 2.1.1 shows the datastructure adopted, while Section 2.1.2 illustrates its second-order cone programming formulation and the iterative iteration procedure implemented to exclude dilation.

2.1.1 JLD datastructure

An assembly can be thought of as composed of blocks that are in contact with each other on surfaces. These are called *interfaces* and are modelled through n-vertices polygons. The JLD method builds upon a graph-based datastructure G(V, E), where data of blocks are stored in the vertices set V, while geometrical and mechanical features of the interfaces in the graph's edges set E [25, 26]. The JLD datastructure is illustrated with respect to the T-shaped block resting on a supporting red base, as depicted in Figure 1a. Standard rigid block analysis (Figure 1b) models the T-shaped block as a single rigid block. At the same time, the datastructure comprises just one edge storing material and geometrical properties related to unilateral contact under the Mohr-Coulomb friction rule (black segment connecting the T-block's and support's centroids). The contact among the block occurs on a *dry interface*. To account for potential internal cracks, JLD discretises the T-shaped block into, e.g. four sub-blocks

in bilateral contact, characterised by finite compressive and tensile strength and a prescribed tangential capacity (**Figure 1c**). The contact among these blocks occurs on *inner interfaces*, shown as red edges in Figure 1. Therefore, this datastructure helps manage the JLD assembly, as illustrated in Figure 1c, which comprises five blocks and five interfaces. In particular, the datastructure accounts for four sub-blocks discretising the original T-shaped block, one support and four inner and one dry interfaces.

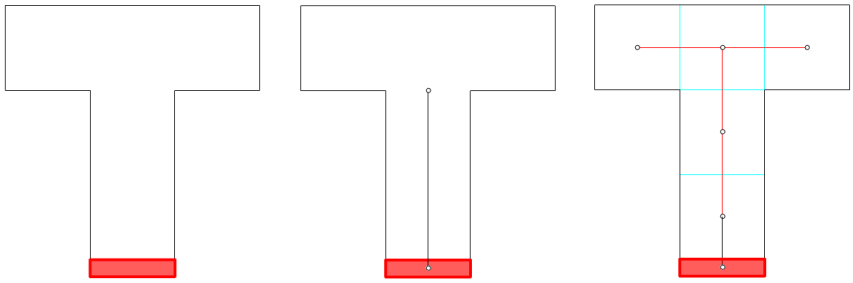

Figure 1: JLD datastructure of a T-shaped block with supporting base: (a) single rigid block on support; (b) standard rigid block datastructure; (c) JLD datastructure considering four inner and one dry interface.

The contact between two adjacent blocks is modelled using a convex formulation [16], which assumes that the interaction occurs at a single point. The internal forces transmitted through this point are represented by a system of forces composed of three forces and three torques along the main directions, applied to the interface's contact point. In the present formulation, the contact point is assumed to coincide with the geometrical centre of the interface. Finally, each interface is associated with an orthonormal reference system with its origin in the interface's geometrical centre, the third axis orthogonal to the interface and the first two lying on the interface.

2.1.2 JLD numerical formulation

Here is briefly illustrated the optimisation problem at the base of the JLD method with respect to a load-bearing capacity analysis where part of the external loads $\mathbf{b}_\lambda$ are linearly incremented till the assembly reaches the collapse using the scale factor λ. The variables of the problem are represented by λ and the internal interface forces:

$$\lambda, \mathbf{N}, \mathbf{V}_1, \mathbf{V}_2, \mathbf{M}_1, \mathbf{M}_2, \mathbf{M}_\mathrm{T}, \tag{1}$$

where $\mathbf{N}$ collects the interface normal force components, $\mathbf{V}_1, \mathbf{V}_2$ denote the interface tangential force components along the first and second axis, respectively; $\mathbf{M}_1$ and $\mathbf{M}_2$ correspond to the interface torques with respect to the first and second interface axes, while $\mathbf{M}_\mathrm{T}$ collects the interface torque components. It is worth noting that the first and second axes refer to the interface's local reference system. With n_{intf} being the total number of interfaces, which sums the number n_{dry} of dry interfaces and the number n_{inner} of inner interfaces, the dimension of each of these vectors is n_{intf}. All these vectors are then stacked into the vector $\mathbf{F}$, whose dimension is $6\, n_{intf}$. The JLD

optimisation problem is formulated as the following second-order cone programming problem:

$$\begin{aligned} \text{Maximise} \quad & \lambda \\ \text{s.t.} \quad & \mathbf{A}_{\text{eq}}\,\mathbf{F} + \mathbf{A}_{\text{b}}\,\mathbf{b} + \lambda\,\mathbf{A}_{\text{b}\lambda}\mathbf{b}_{\lambda} = \mathbf{0} \\ & \mathbf{N}_{\min} \leq \mathbf{N} \\ & |\mathbf{M}_1| \leq \mathbf{M}_{1,\max} \\ & |\mathbf{M}_2| \leq \mathbf{M}_{2,\max} \\ & \sqrt{\mathbf{V}_1{}^2 + \mathbf{V}_2{}^2} \leq \mathbf{T}_{\max} \end{aligned} \tag{2}$$

with:

- λ the scale factor of the external incremental loads $\mathbf{b}_{\lambda}$;
- $\mathbf{F}$ the vector collecting the internal interface forces;
- $\mathbf{A}_{\text{b}}$, $\mathbf{A}_{\text{b}\lambda}$ the linear operators that apply the external loads $\mathbf{b}$, $\mathbf{b}_{\lambda}$ to the centroids of the corresponding blocks, respectively;
- $\mathbf{T}_{\max}$ the vector collecting the interfaces' shear capacity due to the Mohr-Coulomb friction criterion (dry faces) or pure shear resistance (inner faces).

The objective function (2)[1] maximises the scale factor λ in the space of admissible internal stress states defined by the problem's constraints, as detailed below. Equation (2)[2] ensures that the elements are in static equilibrium using the equilibrium matrix $\mathbf{A}_{\text{eq}}$. All remaining inequalities have to be read elementwise. In particular, inequalities (2)[3] ensures that the normal interface forces have to be greater than $\mathbf{N}_{\min}$, which collects the minimum value that the normal force can attain for each interface: 0 for dry interfaces and $-\sigma_t$ A for inner interfaces, with σ_t being the absolute value of the tensile strength of the inner interface and A cross-section area. Similarly, inequalities (2)[4-5] enforces that the absolute value of the bending moment has to be lower than the maximum bending moment the section can withstand, which can be expressed as:

$$\mathbf{M}_{1,\max} = \frac{1}{2}\boldsymbol{l}_2\mathbf{N} - \mathbf{j} * \left(\frac{1}{3}\boldsymbol{l}_2\mathbf{N} - \frac{1}{6}\boldsymbol{\sigma}_t\boldsymbol{l}_2{}^2\right), \tag{3}$$

$$\mathbf{M}_{2,\max} = \frac{1}{2}\boldsymbol{l}_1\mathbf{N} - \mathbf{j} * \left(\frac{1}{3}\boldsymbol{l}_1\mathbf{N} - \frac{1}{6}\boldsymbol{\sigma}_t\boldsymbol{l}_1{}^2\right), \tag{4}$$

with $\boldsymbol{l}_1$ and $\boldsymbol{l}_2$ the two vectors collecting the interface dimensions along the first and second axis, respectively; $\boldsymbol{\sigma}_t$ the vector collecting the interface tensile strength and $\mathbf{j}$ a vector whose i$^{\text{th}}$ entry is zero if the corresponding interface is dry; otherwise, 1. Relation (2)[5] is a second-order cone and ensures that the total shear has to be lower than the interface maximum shear capacity $\mathbf{T}_{\max}$. In particular, referring to the k$^{\text{th}}$ interface and assuming it is dry, it reads:

$$\mathrm{T}_{\max,\mathrm{k}} = \mu \mathrm{N}_k - \frac{1}{\mathrm{c}_{\mathrm{T,e}}}\left|\mathrm{M}_{\mathrm{T,eff},k}\right|, \tag{5}$$

being μ the friction coefficient, while for an inner interface:

$$T_{max,k} = T_{0,k} - \frac{1}{c_{T,k}} \left| M_{T,k} \right| . \quad (6)$$

Using the vector **j**, Equations (5-6) can be combined as:

$$\sqrt{{V_{1,k}}^2 + {V_{2,k}}^2} \leq (j_k - 1) * \left(\mu N_k - \frac{1}{c_{T,e}} \left| M_{T,eff,k} \right| \right) + j_k * T_{0,k} - \frac{1}{c_{T,k}} \left| M_{T,k} \right| , \quad (7)$$

being j_k equal to 1 if inner and 0 if dry. It is worth noting that if the assembly counts n_{intf} the JLD formulation considers $2n_{intf}$ second-order cones because of the absolute value present in (7). As mentioned, the plastic behaviour of a dry joint can result in the distribution of stresses on only a portion of the dry face denoted as *effective area* [16]. The centroid of this area corresponds to the application point of the normal force on the dry face. The shear-torsion capacity of a dry joint with an effective area smaller than the total area of a dry joint is reduced to $M_{T,eff,k}$ which can be found as follows:

$$M_{T,e} - M_T - V_1 l_{2,e} + V_2 l_{1,e} = 0 . \quad (8)$$

The presence of dry interfaces where friction is treated with a Mohr-Coulomb criterion automatically implies that the solution to the limit analysis problem includes dilation whenever sliding is present. To avoid it, this work adopted the iterative procedure proposed by Gilbert et al. [22]. This procedure iteratively solves the equilibrium problem by relaxing the original cone to a quasi-cylinder (using a virtual cohesion and a negligible decreasing virtual friction angle) in the neighbourhood of the solution obtained from the previous step. The resulting flattened surface provides an equilibrium solution with zero dilatancy. The adopted yielding surface for inner interfaces is such that dilation is already prevented. Thus, when used, the iterative procedure applies only to dry interfaces.

2.2 The discrete element method and 3DEC

The Discrete Element Method (DEM) considers the simulated material or structure as a collection of separate solid bodies ("are typically referred to as discrete distinct elements"). DEM numerical techniques have to satisfy the following criteria:

i. The model consists of finite-sized separate rigid or deformable bodies;
ii. The elements can translate, rotate, and deform independently of each other;
iii. The displacements can be large;
iv. The occurrence of new contacts and the loss of existing contacts are automatically tracked together with the modifications of the contact system.

The elements can, consequently, slide relative to one another, partly or completely separate from each other, and form new contacts if the large displacements cause the rearrangement of contact topology. Most DEM codes calculate the motion of the discrete elements with the help of an explicit or implicit time-stepping algorithm: Newton's equations of motion are solved with the help of a time integration scheme (see [27] for more details). The commercial software package named 3DEC is widely used in engineering practice for numerical simulations of the mechanical behaviour

of blocky systems such as rock assemblies or masonry structures. Theoretical details on 3DEC can be found in [27, 28]. In this paper, 3DEC is used to model a discrete assembly as a set of individual masonry blocks consisting of a few perfectly rigid discrete elements glued together with cohesive "inner joints" resisting tension and shear in addition to compression. The masonry blocks, on the other hand, are in dry (i.e. compressive-frictional) contact with each other. both types of inner and dry contacts, the surfaces are subdivided into small sub-contracts. The mechanics of the Coulomb-slip dry joint as well as the inner cohesive contacts, are defined by the following mechanical properties: i) *Normal and shear stiffnesses* show the magnitude of the increment of surface-distributed contact force due to a unit increment in the relative translation in the sub-contact in the normal and tangential directions, respectively; ii) *Strength values* include tensile strength and cohesion. The tensile strength is the maximum possible surface-distributed joint force that the sub-contact can carry in the tensile direction; when reaching this value, the sub-contact breaks due to tension. Cohesion instead specifies the maximal value of surface-distributed shear force that can be transmitted in a sub-contact where zero normal directional surface-distributed joint force is acting. When a nonzero normal force acts in the sub-contact, the maximum allowable shear force is obtained by first multiplying the intensity of the distributed normal force at the joints by the friction coefficient and then adding the resulting value to the cohesion. For contacts being in a frictionally sliding state (either because this is their original type, i.e. dry block-to-block contacts, or because of being an inner face that was broken previously), friction angle shows the usual Coulomb-type initial and residual friction angle; iii) *Friction angle* can apply for both cohesive and dry contacts. iv) *Dilation angle* occurs when the sub-contact slides; thus, the increment of the tangential relative translation is nonzero, resulting in nonzero normal displacement. The ratio between them is proportional to the tangent of the dilation angle.

3 Results

This section shows a few numerical applications of the proposed JLD method. Section 3.1 benchmarks the numerical code and the numerical procedure implemented to avoid dilation against 2D numerical examples proposed in [22], which consider only dry interface. After that, Section 2.2 benchmarks the JLD method on simple examples considering both dry and inner interfaces. Lastly, Section 3.3 proposes the JLD analysis of a flat arch inspired by Leonardo’s arch, validated against a virtual test conducted in the 3DEC environment.

3.1 Validation of JLD single-surface optimisation

Here the JLD numerical formulation is benchmarked against three applications taken from [22]. In particular, the JLD multi-surface optimisation is solved considering only dry interfaces, reducing thus to a single surface plasticity convex approach. In [22], these three examples were also benchmarked against the non-linear formulation proposed by Ferris and Tin-Loi [29]. Each example problem consists of a freestanding wall supported on a base and subjected to in-plane horizontal forces applied to the centroid of each block to simulate earthquake-type loading. Each full block has a

weight of 1 unit, a face area of 4 × 1.75 units, and is subjected to a unit horizontal live load with the same friction coefficient $\mu = 0.65$ was adopted.

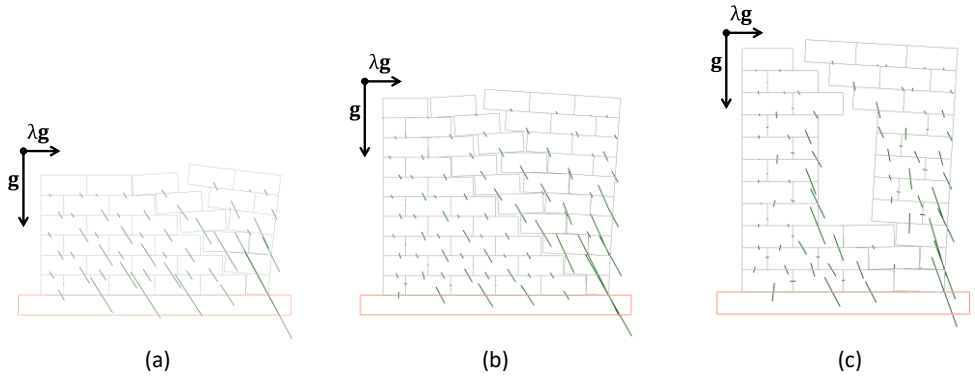

Figure 2: JLD datastructure of a T-shaped block with supporting base: (a) single rigid block on support; (b) standard rigid block datastructure; (c) JLD datastructure considering four inner and one dry interface.

Results are shown in Table 1 and Figure 2. The JLD non-associative friction solutions obtained in the present study are identical to those obtained in [22], both in terms of load factors λ and corresponding mechanisms.

	λ	
Frequency	Gilbert at al.	JLD
(a)	0.63982	0.63916
(b)	0.56262	0.55881
(c)	0.35582	0.35585

Table 1: Comparisons of JLD load-bearing results against the ones proposed in [22].

3.2 JLD multi-surface analysis validation

In this section, the JLD method and its multi-surface formulation are validated using simple examples that can be checked by hand. In all the following analyses, the inner interfaces, whenever present, are characterised by a prescribed shear strength τ coupled with zero tensile strength.

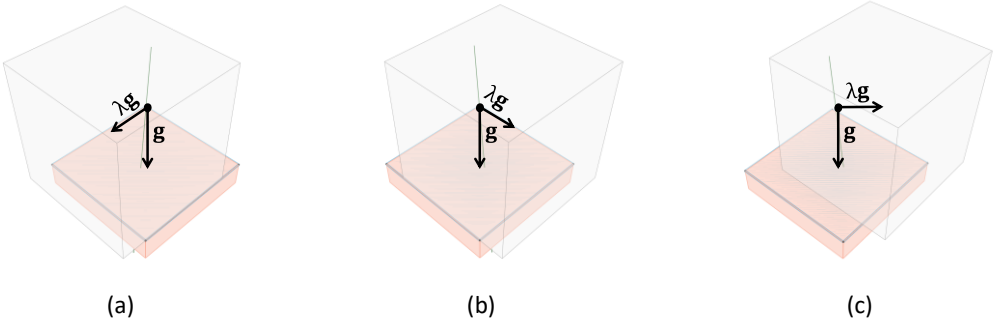

Figure 3: JLD horizontal load-bearing analysis of a simply supported block whose contact with the foundation is supposed to happen on an inner interface. As the reader can notice, the mechanisms are aligned with the incremental forces.

The first example looks at a simply supported block. The contact with the base is defined as an inner interface. The collapse of the assembly always happens independently of the direction when λ equals $\tau A/W$, being A is the inner interface's contact area, and W is the free block's weight (Figure 3). The corresponding collapse mechanisms are aligned with the external force directions. While the first example accounts for only an inner interface, the second one includes both an inner and a dry interface. Indeed, the assembly comprises a vertical block in dry contact with its supporting base. This vertical block is subdivided into two equal stacked cubes with weights equal to W. A horizontal parametric load-bearing capacity is performed, and the results are depicted in Figure 4 as a function of the cube's weight W, the inner interface's shear strength τ, and dry interface's friction coefficient μ.

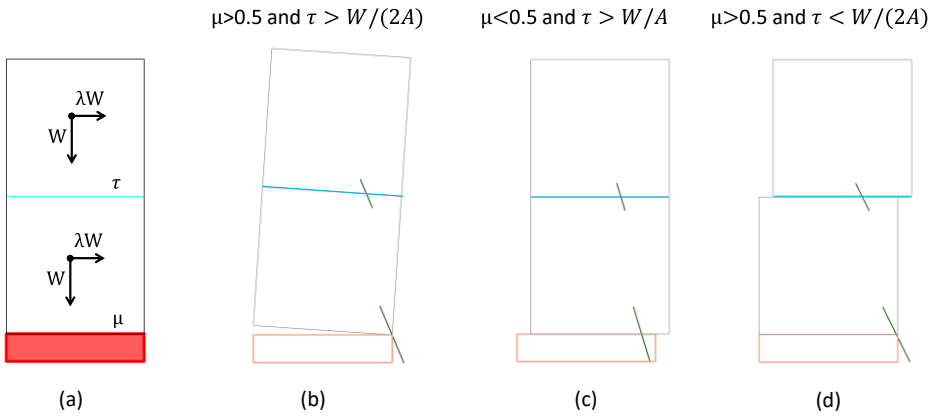

Figure 4: JLD horizontal load-bearing analysis of a block in dry contact with its supporting base and subdivided into two equal stacked cubes: four possible mechanisms as a function of the W, shear strength τ, and friction coefficient μ.

3.3 JLD analysis of Leonardo's flat arch

The last example provided is inspired by Leonardo's arch, which is a flat interlocked arch designed by Leonardo Da Vinci (Figure 5b). The arch modelled in this paper is designed over a discontinuity grid, where each cell has 0.1 m length, width, and depth (Figure 5a).

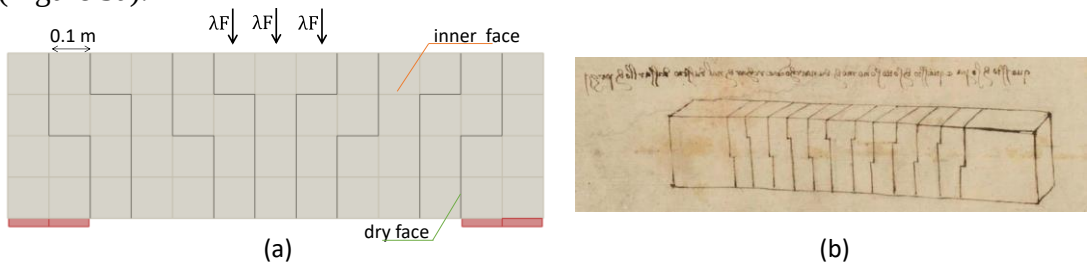

Figure 6: Discretisation and geometry of the flat arch model (a) inspired by Leonardo [30] (b).

The arch is subjected to its self-weight equal to 1400 kg/m^3 and three increasing vertical forces loading the inner rigid block of the arch (Figure 5a). The analysis aims to investigate the potential collapse mechanism and the corresponding collapse by

comparing JLD and 3DEC results. JLD analysis is conducted considering a friction angle equal to 30° for dry interfaces, while inner interfaces are characterised by tangential and tensile strengths equal to 0.2 MPa and 2 MPa, respectively. Figure 7 depicts the corresponding collapse mechanisms found with and without dilation. It is worth noting that the corresponding load multiplier decreases. The 3DEC model consists of the same rigid cells depicted in Figure 6a. Each contact is discretised into a mesh with a maximum edge size of 0.025 m. Table 2 summarises the implemented material properties for both inner and dry contacts. Applying the three increasing forces on the upper face of the middle T-shaped block, the ultimate force for the model with and without dilation at the dry faces is calculated to be 1911.13 N and 2187 N, respectively. Figure 7 shows normal and tangential stresses together with the failure mechanisms. Surprisingly, the 3DEC results provide solutions without dilation that are higher than the ones found with it.

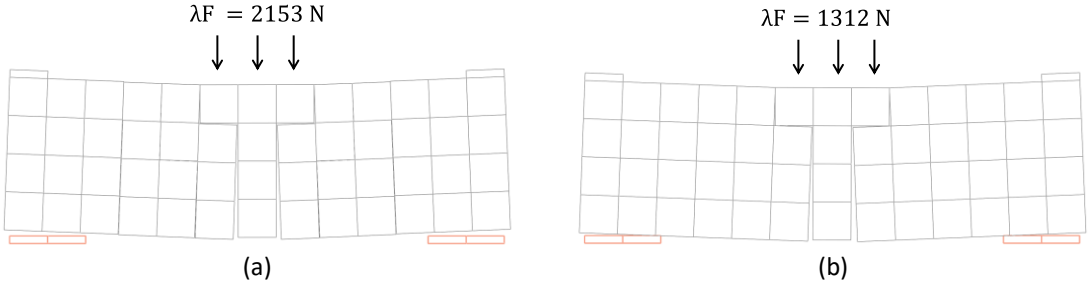

Figure 7: JLD collapse mechanisms with (a) and without dilation (b).

The ultimate values of the model with dilation obtained by JLD (2153 N) and 3DEC (1911.13 N) present an acceptable agreement, while the collapse mechanisms found by the two methods are almost identical. On the other hand, the discrepancy between the results without dilation is not negligible. Indeed, while the JLD result is 1312 N, 3DEC provides 2187 N, which is even larger than the one obtained with dilation. This result is quite surprising as it has been commonly accepted that the load-bearing capacity of a discrete assembly with convex polyhedral blocks reduces when dilation is neglected. This might be extended to assemblies with concave polyhedral blocks, including the presented multi-surface model. However, this conclusion requires a more comprehensive study.

	Normal stiff.	Shear stiff.	Cohesion	Tension	Friction	Dilation
Interfaces	[Pa/m]	[Pa/m]	[MPa]	[MPa]	[°]	[°]
Dry	1.0^9	1.0^9	0.0	0.0	30.0	30.0 and 0.0
Inner	1.0^9	1.0^9	0.2	2.0	0.0	0.0

Table 2: Material parameters adopted for the 3DEC analyses.

4 Conclusions and Contributions

In recent years, the growing interest in low-carbon materials and environmentally friendly joinery methods has driven the development of innovative computational methods to enhance the design of sustainable discrete element assemblies. Dry joints can significantly reduce environmental impact by minimising material consumption

and leveraging sustainable assembly and disassembly processes. However, designing and assessing these assembly typologies requires accurate modelling of complex dry interfaces, including the possibility of block fracturing.

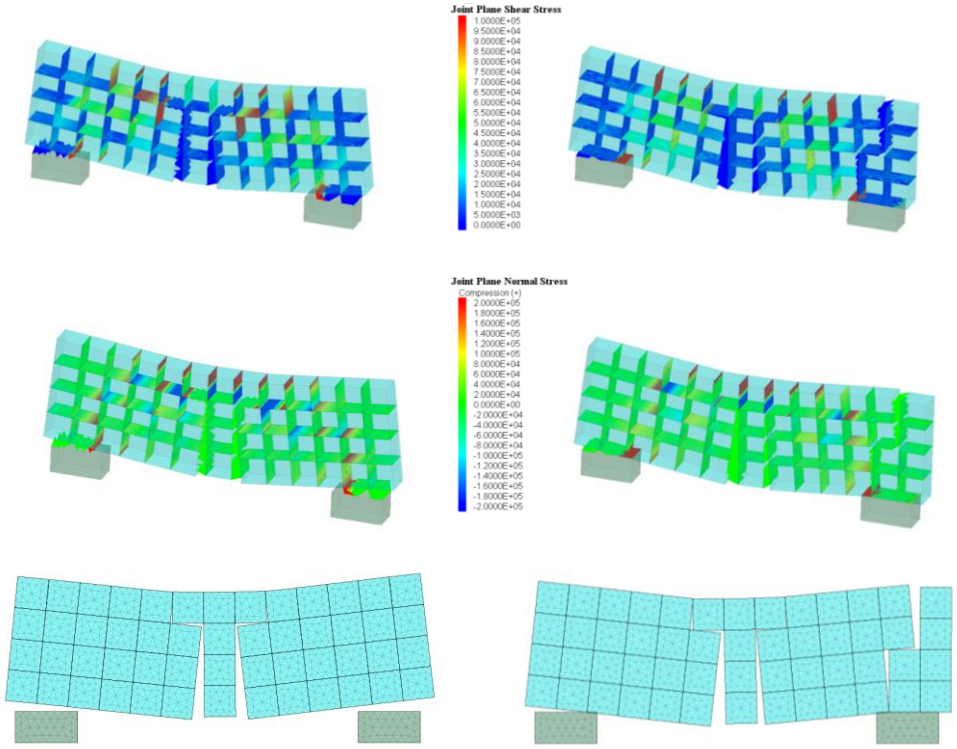

Figure 7: 3DEC results: shear (top) and normal (middle) stresses and collapse mechanisms (bottom) with (left) and without (right) dilation.

To this aim, this research introduced the Joint Layout Design (JLD) method, a new 3D computational approach for modelling and assessing discrete element assemblies with complex-shaped, non-planar interfaces. Unlike standard methods that consider blocks as rigid, JLD accounts for potential internal failures by considering finite internal material strengths in tensile and shear modes. Indeed, the JLD method models potential failure planes within blocks (inner interfaces). In contrast, the contact among original blocks is still assumed to be unilateral and governed by a non-associative Mohr-Coulomb friction law. The mechanical problem is framed within limit analysis, and the corresponding equilibrium problem is solved using iterative second-order cone programming. Collapse mechanisms are defined using dual values from the solution. JLD analyses were first validated against numerical results from the literature without considering inner interfaces. Subsequently, multi-surface JLD analyses were performed and validated manually on a simply supported block. Lastly, the pros and cons of the method were demonstrated through the load-bearing JLD analysis of a flat arch inspired by Leonardo's arch, which was validated against a virtual test conducted in the 3DEC environment. Future works will look at more complex 2D and 3D geometries implementing different yielding surfaces for the inner

interfaces and extending the Gilbert et al. [22] procedure to 3D. Lastly, an in-depth study of 3DEC analyses using inner and dry faces will be performed.

Acknowledgements

The research was funded by the Italian Ministry of University and Research through the Programme “Rita Levi Montalcini for young researchers” (FFO 2020) and by the Hungarian Ministry for Innovation and Technology under grant # NKFI OTKA K-138642.

References

[1] C. Boni, D. Ferretti, E. Lenticchia, "Effects of brick pattern on the static behavior of masonry vaults", International Journal of Architectural Heritage 16(8), 199-1219, 2022. doi: 10.1080/15583058.2021.1874565

[2] O. Gáspár, I. Sajtos, A. A. Sipos. "Friction as a geometric constraint on stereotomy in the minimum thickness analysis of circular and elliptical masonry arches", International Journal of Solids and Structures, 225, 2021.

[3] T. Forgács, V. Sarhosis, K. Bagi, "Influence of construction method on the load bearing capacity of skew masonry arches", Engineering Structures, 168, 612-627, 2018. doi:10.1016/j.engstruct.2018.05.005

[4] H. Pottmann, M. Eigensatz, A. Vaxman, J. Wallner, "Architectural geometry", Computers & graphics, 47, 145-164, 2015. doi: 10.1016/j.cag.2014.11.002

[5] C. Araújo, D. Cabiddu, M. Attene, M. Livesu, N. Vining, A. Sheffer. "Surface2Volume: Surface segmentation conforming assemblable volumetric partition", arXiv preprint arXiv:1904.10213, 2019.

[6] M. Gomaa, W. Jabi, V. Soebarto, Y. M. Xie. "Digital manufacturing for earth construction: A critical review", Journal of Cleaner Production, 338, 2022. doi:10.1016/j.jclepro.2022.130630

[7] A. Kukik, I. Shergil, P. Novikov, "Stone spray project", The Institute for Advanced Architecture of Catalonia, 2012.

[8] WASP, RiceHouse, "The first 3D printed House with earth| Gaia—3D Printers| WASP",URL: 3dwasp.com/en/3d-printed-house-gaia (accessed 5.22. 24) 2018.

[9] WASP, Aït Ben Haddou/clay and 3d printing. URL:3dwasp.com/en/ait-ben-haddou-clay-3d-printing, (accessed 6.13.24), 2024.

[10] S. Bhooshan, V. Bhooshan, A. Dell’Endice, J. Chu, P. Singer, J. Megens, T. Van Mele, P. Block, “The Striatus bridge: computational design and robotic fabrication of an unreinforced, 3D-concrete-printed, masonry arch bridge”, Architecture, structures and construction, 2(4), 521-543, 2022.

[11] M. Rippmann, "Funicular Shell Design: Geometric approaches to form finding and fabrication of discrete funicular structures", PhD diss, ETH Zurich, 2016.

[12] B. Szabó, L. Pásthy, Á. Orosz, K. Tamás, "The investigation of additive manufacturing and moldable materials to produce railway ballast grain analogs", Frattura ed Integrità Strutturale, 2022. doi: 10.3221/IGF-ESIS.60.15

[13] N. Emami, P. Holmquist. "Cast Stereotomy: A material-based investigation of stereotomic modules", (ACSA) 10, 2020. doi: 10.35483/ACSA.AM.108.46

[14] J. Heyman, "The stone skeleton", International Journal of solids and structures 2(2), 249-279, 1966. doi: 10.1016/0020-7683(66)90018-7

[15] R. K. Livesley, "A computational model for the limit analysis of three-dimensional masonry structures", Meccanica 27, 161-172, 1992. Doi: 10.1007/BF00430042
[16] C. Casapulla, A. Maione, "Modelling the dry-contact interface of rigid blocks under torsion and combined loadings: Concavity vs. convexity formulation", International Journal of Non-Linear Mechanics 99, 86-96, 2018. doi: 10.1016/j.ijnonlinmec.2017.11.002
[17] G. T. Kao, A. Iannuzzo, S. Coros, T. Van Mele, P. Block, "Understanding the rigid-block equilibrium method by way of mathematical programming", Proc.Inst.Civ.Eng.:Eng.Comput.Mech. 2021. doi: 10.1680/jencm.20.00036
[18] G. T. Kao, A. Iannuzzo, B. Thomaszewski, S. Coros, T. Van Mele, P. Block, "Coupled rigid-block analysis: Stability-aware design of complex discrete-element assemblies", Computer-Aided Design 146, 2022. Doi: 10.1016/j.cad.2022.103216
[19] E. Mousavian, K. Bagi, C. Casapulla. "Interlocking joint shape optimization for structurally informed design of block assemblages", Journal of Computational Design and Engineering, 9(4), 1279-1297, 2022. doi: 10.1093/jcde/qwac054
[20] P. B. Lourenço, J. G. Rots, "Multisurface interface model for analysis of masonry structures", Journal of engineering mechanics 123(7), 660-668, 1997.
[21] F. Portioli, L. Cascini, C. Casapulla, M. D'Aniello. "Limit analysis of masonry walls by rigid block modelling with cracking units and cohesive joints using linear programming", Engineering Structures, 57, 232-247, 2013.
[22] M. Gilbert, C. Casapulla, H. M. Ahmed, "Limit analysis of masonry block structures with non-associative frictional joints using linear programming", Computers & structures, 84(13-14), 873-887, 2006.
[23] E. Mousavian, C. Casapulla, "Joint layout design: Finding the strongest connections within segmental masonry arched forms", Infrastructures,7,9, 2022. doi: 10.3390/infrastructures7010009
[24] Itasca Consulting Group, Inc. 3DEC — Three-Dimensional Distinct Element Code, Ver. 7.0. Minneapolis: Itasca, 2020
[25] U. Frick, T. Van Mele, P. Block, "Data management and modelling of complex interfaces in imperfect discrete-element assemblies", In Proceedings of IASS annual symposia, 2016(17), 1-9, 2016.
[26] A. Iannuzzo, A. Gesualdo, C. Olivieri, A. Montanino, “3D exploration of internal stresses due to lateral loads and foundation movements in a semicircular arch.” COMPDYN, 2476-2491, 2023, doi:10.7712/120123.10576.21345
[27] J. V. Lemos, K. Bagi, "Discrete element modeling", In Discrete computational mechanics of masonry structures, 189-232. Cham: Springer Nature Switzerland, 2023. doi: 10.1007/978-3-031-32476-5_5
[28] V. Sarhosis, K. Bagi, J. V. Lemos, G. Milani, eds. Computational modeling of masonry structures using the discrete element method, IGI Global, 2016.
[29] M. C. Ferris, F. Tin-Loi, "Limit analysis of frictional block assemblies as a mathematical program with complementarity constraints", International Journal of Mechanical Sciences 43(1), 209-224, 2001.
[30] L. da Vinci 1478–1518 Codex Atlanticus, digital version available online at URL: codex-atlanticus.it